8844 *Macromolecules* **2009**, *42*, 8844–8850
DOI: 10.1021/ma9017394

Macromolecules
ARTICLE

Small Molecule Segregation at Polymer Interfaces

E. Sivaniah* and R. A. L. Jones†

Cavendish Laboratory, Cambridge University, Cambridge CB3 0HE, U.K.

David Higgins

Higgins Consultancy Ltd., Whiteleyside, Commondale, Whitby, N. Yorks, YO21 2HJ, U.K. †Present address: Department of Physics, Sheffield University, Sheffield S3 7RH, U.K.

Received August 4, 2009; Revised Manuscript Received September 13, 2009

ABSTRACT: The segregation behavior of a small molecule plasticizer additive at an immiscible polymer−polymer interface was explored. Deuterated and nondeuterated plasticizer, benzylbutyl phthalate, were added to bilayer and multilayer thin films of polystyrene (PS) and poly(methyl methacrylate) (PMMA), and the resulting interfacial structure was analyzed by direct and indirect depth profiling techniques, using nuclear reaction analysis and neutron reflectometry, respectively. In the latter, contrast matching of the two polymer components together with a multilayer sample was used to enhance the scattering cross-section depth profile due to small molecule interfacial segregation and thus provide greater sensitivity to small amounts of interfacial segregation. The results indicated a larger-than-expected segregation of the additive to the polymer interface and consequently a greater degree of compatibilization of the PS−PMMA interface.

1. Introduction

The control of the strength of polymer−polymer interfaces is desirable in many industrial applications including coatings and polymer blends.[1−3] Copolymers are a principal agent for improving interfacial adhesion but are considerably slower than small molecule counterparts to migrate to polymer interfaces.[4] This can be crucial in industrial processes where the majority of strength development is required to take place in a relatively short amount of time. From an academic point of view, studies of polymeric adhesion modifiers are simplified by their relative stability under scrutiny or during preparation. Moreover, interfacial phenomena are more easily measured in the larger macromolecular systems with subnanometer precise neutron and X-ray scattering techniques.[5] In this paper we will discuss the interfacial behavior of polymer interfaces that are modified by small molecular components, where several of these experimental advantages are lost and more elegant experimental methods are called for. Such small molecular additives, especially plasticizers, are widely used in industry (e.g., coatings and blends).

Consider a ternary system of polymer (A)/polymer (B)/solvent (S) where the polymer phases are immiscible and the solvent phase has limited miscibility with both polymers. In such cases, it is intuitive that small molecules segregate to an incompatible polymer interface. Because of the smaller entropic penalty involved with a polymer−solvent interface, the three-component system might evolve into two almost pure polymer phases separated by an interface consisting primarily of small molecules.[6] However, there is also an entropic penalty if all the solvent is localized at the interface. A compromise is achieved whereby the solvent distributes itself uniformly within the system and still achieves an excess at the interface. Thus, entropy is the dominating influence in solvent-based ternary polymer systems in contrast to copolymer modified blends, where enthalpic interactions have a stronger influence in determining the nature of copolymer interfacial segregation.[7]

*To whom correspondence should be addressed. E-mail: es10009@cam.ac.uk.

The determination of the interfacial profile of the three-component system is based on minimization of the path along the system free energy surface as one traverses the composition profile from one majority polymer phase to the other. This potential surface contains the Flory−Huggins thermodynamic free energy of mixing and also a component associated with composition gradients. The latter term is most simply expressed by a square gradient approximation and is described in many papers discussing multicomponent systems.[8−13] In particular, Lifshitz and Freed discuss compressibility effects on interfacial width by including vacancy sites in a binary polymer melt.[10] This has several similarities to the ternary polymer/polymer/solvent system. Generally ternary systems are further complicated by asymmetric polymer−solvent interactions that require numerical solutions to the interfacial composition distribution problem. Numerical approaches to self-consistent mean-field theory (SCMF) that described this system require the solution of two simultaneous modified diffusion equations (MDE) for the partition functions of two of the polymer species in the ternary mixture.[7,14] While the application of SCMF theory has largely been to macromolecular systems (where the effects of fluctuations are lessened) both Hong and Noolandi[14] and Helfand and Tagami[6] have considered the effects of a small molecule component on binary polymer interfaces. Helfand and Tagami, by introducing a compressibility term, were able to formulate expressions for the polymer interfacial profile in the presence of a solvent.[6] Their expression, assuming a symmetric polymer interface, can be used to predict the extent of the excess interfacial segregation of solvent as $\phi_{s,excess}(x) = 1 - \phi_{s,bulk} - \phi_A(x) - \phi_B(x)$ where $\phi_A(x) = \phi_B(-x)$ and where

$$\frac{\phi_A(x)}{\phi_{A,bulk}} = \frac{\xi^2}{1+\xi^2}\left\{\left[1+\chi\left(\frac{\sigma_\chi}{b}\right)^2\frac{1-\xi^2}{(1+\xi^2)^2}\right] - \frac{\chi}{\zeta}\left[\frac{3(1+7\xi^2)}{8(1+\xi^2)^2}+\frac{\chi}{12}\left(\frac{\sigma_\chi}{b}\right)^2\frac{(4+111\xi^2-243\xi^4+80\xi^6)}{(1+\xi^2)^4}\right]+\ldots\right\} \quad (1)$$

 Published on Web 09/30/2009

where

$$\xi = \exp[(6\chi)^{0.5})x/b]$$

and

$$\chi = (\chi_{AB} + \chi_{AS} - \chi_{BS})\phi_{A,bulk}$$

and

$$\zeta = [(1 - \phi_{A,bulk})^{-1} - 2\chi_{AS}]\phi_{A,bulk}$$

In this expression, ϕ is the volume fraction and x refers to the distance from the defined polymer interface. b and σ_χ are the Kuhn length and a characteristic dimension associated with nonlocal chain effects, taken as 7 and 5 Å, respectively. χ is the effective interaction parameter and is a function of the pair interaction parameters for the ternary components (A, B, and S). It can be seen for the analytically simple but physically unlikely situation of a neutral solvent ($\chi_{AS} = \chi_{BS}$) that the solvent simply dilutes the polymer interaction parameter χ_{AB}.

For symmetrical solvent−polymer interactions ($\chi_{AS} = \chi_{BS}$) and polymer−polymer interactions ($\chi_{AB} = 0.1$, $\phi_{S,bulk} = 0.1$), this leads to an integrated interfacial excess, x^* [$\equiv \int_{-\infty}^{\infty}(\phi_s(x) - \phi_{s,bulk}(x))\,dx$], of ~0.01 Å. By contrast, typical excesses for copolymer interfacial excesses are in the order of 1−10 nm.[15] Hong and Noolandi showed that the polymeric interfacial width, α, increased in the presence of a neutral solvent as $\alpha_{A,B,S} = \alpha_{A,B}(1 - \phi_{S,bulk})^{-0.5}$ where α_{AB} is the pure A/B polymer interface width.[14] For our typical values, this represents a 5% increase in interfacial width. It is perhaps these small effects that have dissuaded experimental verification of the solvent segregation phenomenon.

In this paper, we report on such measurements in a ternary polymer/polymer/small molecule system and compare these to predictions of solvent-induced interfacial broadening and solvent segregation. We employ a classical binary polymer system of polystyrene (PS) and poly(methyl methacrylate) (PMMA) to which is added a well-known industrial small molecule plasticizer, benzylbutyl phthalate (BBP).

2. Experimental Details

2.1. Materials. Benzylbutyl phthalate (BBP), a liquid at room temperature with a relatively high boiling point (370 °C), was purchased and used as-is from Sigma-Aldrich. Deuterated BBP (dBBP) was used to carry out nuclear reaction analysis experiments. Since commercially available dBBP was only slightly (4 out of 20 possible substitutions) labeled, a nearly completely deuterated dBBP (16 out of 20 possible substitutions) was synthesized and purified to 98% following the original chemical recipe provided by the Monsanto Corp.[16] Anionically synthesized, normal and deuterated polystyrene [PS] and poly(methyl methacrylate) [PMMA] of low polydispersity ($M_w/M_n < 1.06$) obtained from Polymer Source were used. The molecular weights employed were generally large (PS; $M_w = 630$K, 1.5M; (d)PMMA $M_w = 330$K or 314K).

2.2. Plasticizer Characterization. In early experiments it became clear that despite the relatively high BP of the plasticizer, it was prone to evaporate from PS or PMMA thin films at the typical annealing temperatures (i.e., > 100 °C). This was confirmed quantitatively by measuring the shrinkage of polystyrene films that initially contained 23% (volume fraction) of BBP using spectroscopic ellipsometry to determine the polymer film thicknesses as the initially plasticized polymer films were annealed (Figure 1a, inset). Taking the initial slopes of this shrinkage data, the rate of shrinkage as a function of temperature (Figure 1) can be determined.

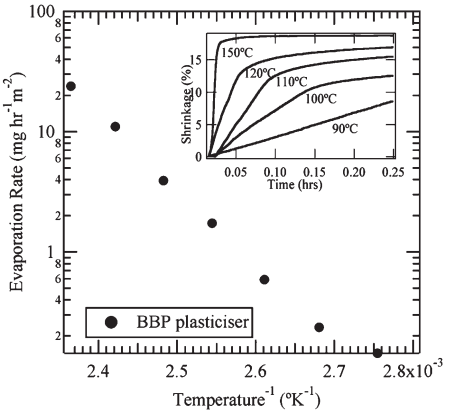

Figure 1. Evaporation rates of BBP from a PMMA film show as a function of inverse temperature. Inset shows the deswelling of BBP/PMMA films (23 wt % fraction BBP) during annealing in air at various temperatures.

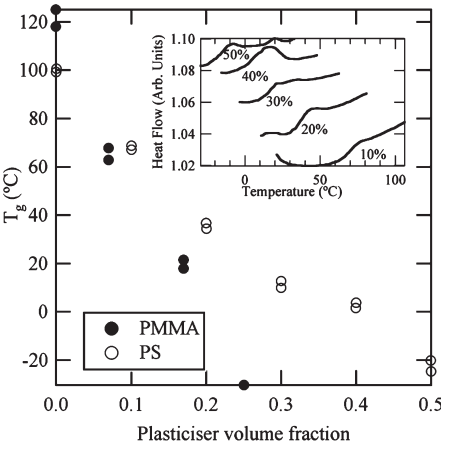

Figure 2. Depression of the glass transition temperature in plasticized PS and PMMA (inset shows DSC analysis for given % of BBP in PS).

The plasticization effect of BBP on bulk polymer samples was determined using differential scanning calorimetry. Samples were prepared by dissolving both BBP and polymer in a common solvent (toluene) to the proportions required. Once homogeneous the solvent was allowed to evaporate from the mixture. Residual solvent was removed by leaving the sample in a low-vacuum oven at 80 °C for 1 day. The depressed glass transitions for PS and PMMA are given in Figure 2 (with DSC scans in the inset) as a function of the plasticizer content. Clearly, the T_g is significantly reduced by the addition of BBP; both PS and PMMA become rubbery for BBP fractions exceeding 20−30%.

2.3. NRA Sample Preparation, Instrumentation, and Analysis. PS−PMMA bilayer samples containing BBP were prepared. First, a 200 nm thick PS (M_w 630K) film was spun-cast (from a toluene solution) onto a hydrofluoric acid-etched silicon wafer. Then a 220 nm thick PMMA (M_w 330K) film containing dBBP was spun-cast onto glass and subsequently floated on top of the polymer sublayer. The films were prepared a week in advance for NRA analysis to allow dBBP diffusion into the underlying PS layer.

The Nuclear Reaction Analysis (NRA) facility at Surrey University (Guilford, UK) was used to determine the composition profile of dBBP in the bilayer films. The technique involves probing the composition profile of a deuterated species using a beam of monoenergetic helium ions (^{3}He).[17] By employing a beam of moderate energy (−0.7 MeV), a resonant nuclear reaction is possible between helium ions, ^{3}He, and deuterons,

producing protons and ^{4}He ions. The energy of the reaction products can be calculated using momentum and energy conservation. This is related to the ^{3}He energy loss as it traverses a path through the sample prior to colliding with a deuteron. Thus, quantitative depth profiling is based on the unequivocal relationship between the energy of the emergent reaction products and the depth at which the reaction occurred.

The ^{3}He beam, produced by a Van de Graff accelerator, impinges on the sample in a vacuum chamber (2×10^{-5} Torr). The sample holder has an internal coldfinger arrangement to freeze samples that are particularly susceptible to beam damage or, in our case, plasticizer evaporation. A load-lock attachment to the chamber ensures quick sample changeover times without bringing the entire chamber back up to atmospheric pressure.

The exiting protons are collected by an Ortec silicon surface barrier detector and analyzed by a multichannel analyzer (MCA). The result is an output of proton counts vs channel number. Channel numbers are transformed into depth using known stopping powers of the polymer media and the energy loss per channel. The latter is calibrated using internal radioactive alpha sources within the sample chamber, and the stopping powers can be found in the literature.[18] The proton counts are normalized using raw data from a uniformly deuterated sample of the same density, thus obtaining the composition profile of the deuterated species.

2.4. NR Sample Preparation and Analysis. Neutron reflectometry is widely accepted as the most accurate current means of providing quantitative compositional information at surfaces and interfaces. NR relies on a scattering contrast, making it sensitive to regions where the neutron scattering length varies sharply.[5] The advantage of NR (for the investigation of polymeric systems) over the almost analogous technique of X-ray reflectometry lies in the use of deuterated isotopes to achieve a scattering contrast with a typically insignificant effect on the thermodynamics of the system. A time-of-flight reflectometer beamline [CRISP] and the spallation neutron source at the Rutherford Appleton Laboratories were used in our experiments.

Given the propensity of the BBP to evaporate from annealed thin films, an alternative method for incorporating the plasticizer into the polymer films was used for samples studied with neutron reflectometry. This was to prepare the polymer films on silicon wafers prior to annealing them under reduced pressure in an atmosphere containing the plasticizer. A simple sample chamber was constructed that contained the unplasticized polymer films and also a tank of 5−10 g of BBP plasticized (50 wt %) PS. The sample chamber was evacuated to known initial pressures and then placed in an oven at 175 °C for a day before being cooled to room temperature. Plasticizer was absorbed into the polymer films from a saturated gaseous condition; the plasticizer content in the film was systematically altered by control of the initial pressure in the sample chamber. Quantitative determination of plasticizer content was subsequently possible by neutron reflectivity analysis.

Four sample types were annealed in the chamber for the NR experiment. Single layers of dPS (50 nm) and dPMMA (50 nm) were used to measure the amount of BBP adsorption. A dPS (50 nm)−PMMA (100 nm) bilayer was used to investigate BBP sorption effects on interfacial broadening.

A more complex sample geometry was used to measure plasticizer segregation. Multilayers of 10 alternating dPS and dPMMA layers, each 50 nm thick, were made. The dPMMA films contained a small amount of PMMA (5%) so that its scattering length density matched that of dPS. This in principle created a contrast-matched multilayer film where the only scattering contrast apparent to the neutrons occurred at the air/polymer and polymer/substrate. As a result, a reflectivity profile for this system would correspond to that of a 500 nm deuterated PS film, characterized by resolution-damped high-frequency Keissig fringes. Relatively high molecular weight polymers (dPS, 1.5M; dPMMA, 314K; PMMA, 330K) were used for these neutron samples to avoid dewetting of the multilayers. This molecular weight mismatch was not considered to have a significant effect on the interfacial properties of the system.[19] The concept of this arrangement was that plasticizer adsorbed preferentially at the dPS/dPMMA interfaces would result in periodically spaced scattering holes within the multilayer. The periodic combination of these scattering holes should lead to a Bragg-like scattering shoulder in the reflectivity data. Such manipulation of contrast in neutron scattering samples can be a powerful method to increase the amount of information extracted.[20,21]

The typical method for fitting reflectivity data is by trial and error. On the basis of other evidence, such as real space profiles from NRA, a functional form for the composition profile and hence scattering length density profile for each of the species is "guessed". The corresponding reflectivity profile is calculated via the optical matrix method (OMM),[22] and model parameters are suitably adjusted until satisfactory convergence of data to fit is achieved. We used an additional method for data fitting to provide a bias-free suggestion for the distribution of plasticizer in the multilayer films. This method is based on a free-form fitting approach to our data using a maximum entropy method, MaxEnt.[23] The algorithm discretizes the sample profile, the thickness of which is known, and varies the composition of the resulting segments. Therefore, with typically many more variables than data points, the resulting real-space profile has the potential to have no physicality. However, the MaxEnt method is particularly strong at being able to suggest real-space composition profile to data where the distribution of components is relatively unique. This is for example the case when MaxEnt is used to suggest the best real-space fitting to the reflectivity data of a series of alternating deuterated and nondeuterated polymer layers, as described in our earlier work.[24] The typical, bias-free, inputs for fitting reflectivity data with MaxEnt are the sample's average scattering length density and the total sample thickness, which can be determined in advance with ellipsometry.

3. Results and Discussion

3.1. Analysis of NR Results. In the final analysis, two definitive NRA samples were prepared which initially contained 20 or 30% (volume fraction) of dBBP in PMMA on a PS substrate. The NRA data for these are shown in Figure 3. The raw data were normalized by a thick deuterated PS sample profile and subsequently by conserving the total amount of dBBP in the bilayer to the initial amount present in the upper PMMA layer. Figure 3a,b shows a perceptible segregation of dBBP at the PS−PMMA interface which is now ∼120 nm from the air surface. Since the original film was about 250 nm thick, this can imply that as the plasticizer diffuses into the PS film, there is shrinkage of the original PMMA film. However, as can be seen in the data, the BBP clearly does not extend throughout both films (since the total bilayer thickness is ∼450 nm) and has not yet reached equilibrium. This will also explain the extended dBBP profile that tails deeper into the film, in comparison to the relatively sharp front edge (at depth = 0 nm). A difficulty in interpreting this data arises since one cannot monitor both the position of the polymer interface and the diffusing component.

A trilayer model (shown in Figure 4) was used to fit the data. This described the BBP volume fraction within the PMMA layer, the sublayer, and in an intermediate layer used to account for BBP interfacial segregation. For comparison, a single layer fit, describing a uniform plasticizer distribution, was also applied to the data. The edges of these layers were convoluted with a Gaussian distribution, the fwhm of which can be used as an indication of the sharpness of the profile. The trilayer dimensions for the fits are given in

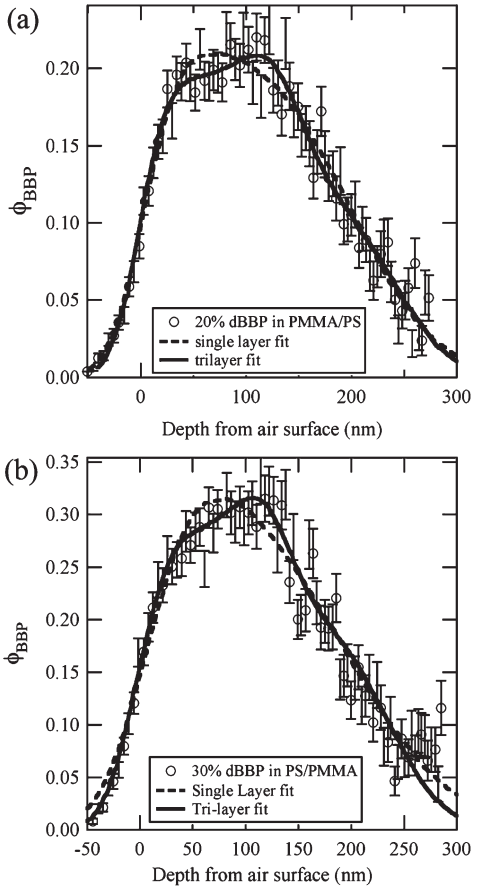

Figure 3. NRA profiles for dBBP in PMMA/PS bilayers where the dBBP content is (a) 20% and (b) 30%. Also shown are single (dashed line) and trilayer (solid line) fits as described in the text.

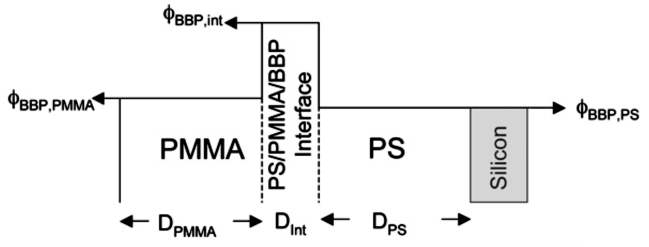

BBP content	D_{PMMA}, $\phi_{BBP,PMMA}$	D_{int}, $\phi_{BBP,int}$	D_{PS}, $\phi_{BBP,PS}$
20%	122nm, 0.19	14nm, 0.38	105nm, 0.12
30%	119nm, 0.29	16nm, 0.49	107nm, 0.21

Figure 4. Trilayer model fit parameters used to fit the data shown in Figure 3. With the exception of the air−polymer interface, the model was convoluted with a Gaussian smoothing function with a full width at half-maximum (fwhm) of 50 nm. The front edge fwhm value was 25 nm.

Figure 4, and the convolution width of the blocks deep into the sample was −50 nm whereas the fwhm at the front edge of the sample was ∼25 nm. A physically sharp interface is expected to be fit by a fwhm value of ∼15 nm. This suggests there was some removal of BBP from the front of the sample, despite the use of the cryo-stage.

Plasticizer segregation at the interface is expected to occur over a distance of a few molecules. Hence, no quantitative information is expected from the NRA data. Instead, the fits indicate that there is a segregation peak at the polymer−polymer interface, the precise height and width of which are

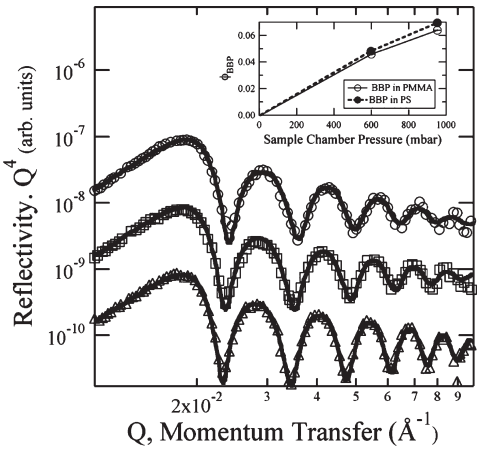

Figure 5. Reflectivity data for single layers of dPS exposed to no plasticizer (circles) and a plasticizer environment produced in a chamber pressure of 600 mbar (squares) and 950 mbar (triangles). The fitted data indicate a shift in the critical edge of the NR profiles and are used to determine the amount of BBP adsorbed into the films (see inset).

shrouded within the resolution envelope of the ion-beam technique. The fits also show a relatively small amount of BBP penetration into the polymer sublayer despite the time allowed for equilibration. A concern in data interpretation is the uncertainty of the sample front edge, since it is plausible that some dBBP will have evaporated from the surface. Therefore, the NRA analysis provides some evidence, but not nearly convincing enough, of segregation at the PS/PMMA interface. It is necessary to use a higher resolution method, neutron reflectometry, to prove more conclusively that this is occurring.

3.2. Analysis of NR Results. Plasticizer sorption into different samples of single layer deuterated films was correlated to the shift in the position of the reflectivity data's critical edge (the Q value below which total external reflection occurs). This shift can be seen in Figure 5 to lower Q (momentum transfer) values for higher BBP adsorption. OMM fits for samples of dPS in three different BBP atmospheres were obtained using a single layer model with a fitted uniform scattering length density (Figure 5). Since this density is linearly related to the fraction of BBP and deuterated polymer present, the resulting BBP adsorption can be calculated as shown in the inset of Figure 5. This data indicates typical values of up to 7% BBP content in the films in a manner linearly dependent on the initial chamber pressure.

A similar adsorption of BBP into layers of dPS and dPMMA was measured. In order to correlate the adsorption at all chamber pressures, an interpolation of the mean uptake into both polymers is used from Figure 5.

Figure 6 shows the reflectivity profiles from four contrast matched multilayers. The unannealed unplasticized sample provoked the greatest surprise. Instead of a monotonically decreasing reflectivity profile synonymous with a thick uniformly deuterated polymer layer, peaks were observed at periodic Q-spacings. Such a profile was expected for plasticizer segregation at the interfaces of the multilayer elements. This was confirmed by data fitting with MaxEnt using a uniform scattering profile as an initial guess. Since MaxEnt uses two reference scattering length densities (of dPS and PS), changes in scattering length through the sample are related to the volume fraction of the deuterated species (Figure 7). The MaxEnt fits clearly show periodic drops in polymer composition at roughly 50 nm spacings (indicated by arrows in the figure). The fact that these peaks are largest

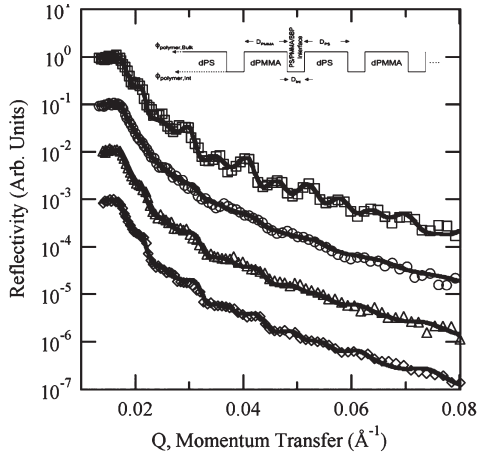

Figure 6. Reflectivity data and fits (using OMM) for contrast matched dPS/dPMMA multilayers. The schematic of the comb profile fitting model is given in the inset. Data are shown for as-made unplasticized, multilayers (squares), annealed unplasticized multilayers (circles), and annealed multilayers exposed to a plasticizer environment produced in a chamber pressure of 600 mbar (triangles) and 950 mbar (diamonds).

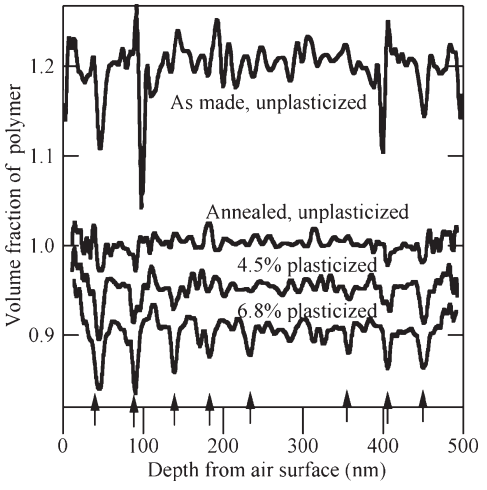

Figure 7. Maximum entropy-based free-form fits for contrast matched dPS/dPMMA multilayers. The data are described in the text and within the figure. The arrows indicated are the putative locations of the polymer interfaces where excesses of plasticizer are observed.

near to the ends of the samples is artificial since similarly good fits are possible when the relative positions of these peaks are rearranged.

The scattering deficit at the interfaces of the unannealed unplasticized multilayer was unexpected. However, the composite layers are in an as-spun state and likely to have a density variation between the interface and the bulk. Additionally, contaminant particles, such as water molecules, trapped at the interface during multilayer fabrication will have the effect of locally reducing the scattering length density. On annealing the unplasticized multilayer sample, both these effects are removed, as seen in the reflectivity data (Figure 6) and corresponding MaxEnt fits (Figure 7).

The MaxEnt profiles fits to data from multilayers that were subject to a plasticizer atmosphere once again reveals a decrease in the mean scattering length density of the sample indicating BBP uptake. More crucially the MaxEnt profiles indicate a re-emergence of the scattering holes at the interface.

These results suggest an inverted comb profile with which to quantitatively fit the data using the OMM. The relevant

Table 1. Fitting Parameters Extracted from NR Analysis of Multilayer Samples

contrast matched multilayer samples	D_{dPMMA}, D_{dPS}, D_{int} (nm)	$\phi_{s,bulk}$, $\phi_{s,int}$	interfacial width, α (nm), interfacial excess,[a] x^* (nm)
0% unannealed	43.0, 49.0, 2.3	0.01, 0.14	1.25, −0.32
0% annealed	42.6, 45.0, 2.3	0.00, 0.04	1.25, −0.09
ϕ_s = 0.04 annealed	41.2, 46.1, 2.2	0.03, 0.11	4.0, 0.24
ϕ_s = 0.07 annealed	41.3, 46.9, 1.8	0.05, 0.14	3.5, 0.25

[a] Determined from integration of fitted interfacial profile.

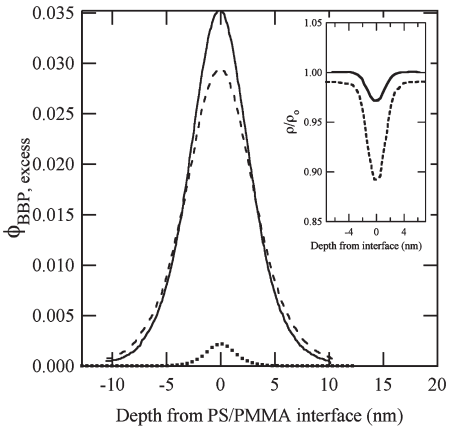

Figure 8. Convoluted interfacial segregation profiles from comb model fitting of multilayer samples. The inset shows the relative density of polymer for the unannealed (dotted line) and annealed (full line) unplasticized multilayers. The main figure shows the excess interfacial plasticizer volume fraction profiles for multilayers with a bulk plasticizer content of ϕ_s = 0.04 (dashed line) and ϕ_s = 0.07 (full line) and the predicted interfacial excess using eq 1 for the typical parameters used in this paper (dotted line).

fitting parameters, shown in Figure 6, are the two bulk polymer thicknesses, D_{dPS} and D_{dPMMA}; a characteristic width, D_{int}, over which plasticizer segregation occurs; and the plasticizer volume fractions in these regions, $\phi_{s,int}$ and $\phi_{s,bulk}$. The Gaussian roughness of the layer interfaces was an additional parameter and, entered via a Debye−Waller factor, is used to smooth the artificially sharp model interfaces of the comb model. Good fits to the data using this model are given in Figure 6, and the corresponding fitting parameters are shown in Table 1. From Table 1, it is clear that BBP has been adsorbed into the annealed multilayers exposed to a BBP atmosphere; the amount adsorbed and segregating at the interface increases at a higher plasticizer atmosphere. It should be noted that the data fit values of $\phi_{s,bulk}$ in Table 1 differ slightly from the values of these multilayers are labeled with in column one. The labeled values of ϕ_s come from single layer reflectivity samples (e.g., Figure 5) and are considered more accurate. A more detailed segregation profile at the interface is found using the convolution of the plasticizer segregation layer (from the comb model) with the experimentally extracted roughness values (Figure 8). The main figure indicates the interfacial excess volume fraction of BBP (above that of the bulk) and can be used to calculate the total plasticizer interfacial excess, x^*. The calculated excesses are also listed in Table 1 for both unplasticized and plasticized multilayers and are much larger than the Helfand and Tagami expressions calculated earlier. This is also apparent when comparing the convoluted profiles in Figure 8 to a plot of eq 1. The inset to Figure 8 also includes a plot of the local density profile, ρ, of the polymer multilayers prior to and after annealing. Here ρ_0 is assumed

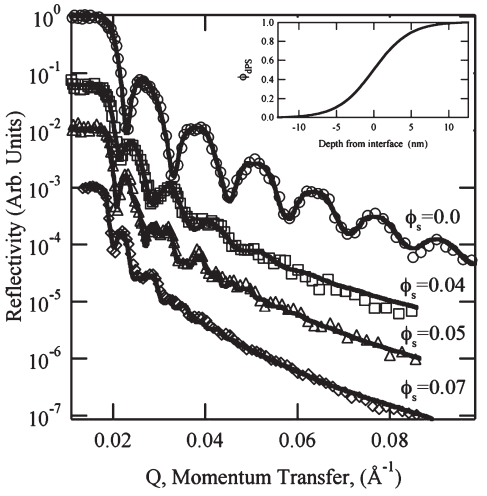

Figure 9. NR data and fits (using OMM and tanh profile) of four bilayer samples. The samples contain no plasticizer (circles) and some plasticizer; $\phi_s = 0.04$ (squares), $\phi_s = 0.05$ (triangles), $\phi_s = 0.07$ (diamonds). The interfacial detail of the tanh profile for the $\phi_s = 0$ case ($\alpha = 4.8$ nm) is given in the inset.

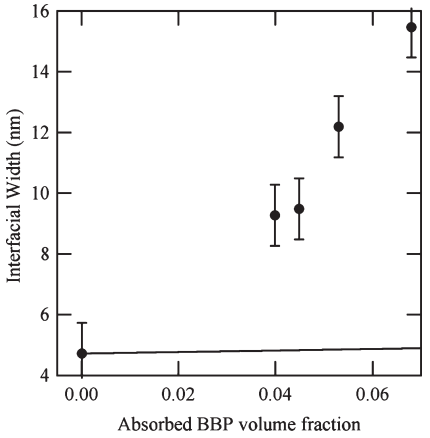

Figure 10. NR determined interfacial widths, α, obtained from bilayer samples. The figure also shows (as a line) the expected interfacial width as predicted by Hong and Noolandi.

to be equivalent to the equilibrium density that is achieved after the multilayers have been annealed into their melt state and allowed to reach equilibrium chain conformations. The data are interesting in that it indicates two things. As expected, the surfaces of the polymer films prior to annealing are less well packed, and in fact the overall film is less well packed than an annealed bulk film. The second point is that even after annealing the polymer interfacial chain packing is less than in the bulk.

Bilayer NR data (a selection of which are shown in Figure 9) indicate, through the loss of Keissig fringes at high Q values, the broadening of the polymer interface on exposure to BBP vapor. These data were fit (see Figure 9) using the OMM with the archetypal hyperbolic tangent profile, $\tanh(x/\alpha)$, where α is used to characterize the interfacial width. For bilayers with no plasticizer, the data fits return the interfacial width value 4.8 nm, in broad agreement with previous work.[25,26] As seen in Figure 10, there is a general increase in the interfacial width, α clearly correlated with the amount of BBP adsorption in the bilayers. Also shown is the HT-predicted interfacial width for the system $\alpha_{A,B,S}$. Again there is an order of magnitude difference between the experimentally observed interfacial effects and that predicted by simple theory.

3.3. Conclusions. In spite of the problems that arise from this particularly difficult experiment, there have been several notable findings. It was possible to control the amount of plasticizer absorbed to a reasonable extent. This has been shown through the relative increases in film thicknesses measured using ellipsometry and reflectometry as well as through the decrease in overall scattering power of deuterated polymer films. From this we are able to make definite conclusions about BBP segregation at the PS−PMMA interface. Such conclusions have also ruled out other possible causes of the behavior seen with NR. Annealing of unplasticized contrast matched multilayers removed the interfacial defects that caused scattering deficits at the interface in unannealed samples. Thus, the regrowth of scattering holes, in samples annealed in a BBP atmosphere, can only be ascribed to segregation of the plasticizer at the polymer/polymer interfaces.

BBP surface segregation and evaporation are very likely to occur to a small extent and will begin from the moment the samples are taken from the preparation chamber. The multilayer geometry was designed to minimize this effect by containing many interfaces. Significant surface segregation would also have been visible from the reflectivity profiles taken from adsorption to single polymer layer samples, whereas our data were adequately fit with a uniform composition profile.

Another explanation for the disappearance of the reflectivity fringes from the dPS−PMMA bilayers is that surface roughening and not interfacial broadening is occurring. However, control of both surface and interfacial width parameters during the fitting procedure negated this possibility; surface roughnesses were consistently found to be ∼1 nm.

The experimentally observed phenomena, while qualitatively predictable, disagree with the currently available theoretical expectations by an order of magnitude or more; specifically, experimentally determined integrated excesses are $\sim 10^{-1}$ nm compared to the predicted 10^{-3} nm from mean-field theory. Equally, changes in interfacial width are seen to be more sensitive to the addition of plasticizer than what is expected from theory (see Figure 10). Some qualifications must be made for the use of the HT expression since it models the plasticizer as a neutral diluent of the interaction between the polymer segments.[6] The extent to which asymmetry affects the prediction is not easily calculated. Moreover, it is a difficult task, from this data, to ascertain the relative position of the BBP-rich interface with respect to the two polymers since the small amount of segregation makes little difference to the interfacial scattering profile when contrast matching is not used and the interface is effectively invisible when it is used. It has been assumed, on the basis of BBP adsorption into single polymer films, that our system is fairly symmetric and the solvent approximately neutral. However, it may be that our data can be compared to recent models put forward by Wang and Sanchez, who specifically looked at supercritical CO_2 effects on a polymer interface[27] and includes the asymmetric relationships between the system components.

4. Summary

After characterization experiments on some properties of BBP were performed, nuclear reaction analysis (NRA) and neutron reflectometry (NR) were used to obtain composition profiles of the plasticized polymer interface. Early studies showed that plasticizer volatility in thin polymer films seriously affected the interpretation of experimental data. Nonetheless, NRA revealed

real space evidence of plasticizer interfacial segregation that supported more quantitative results obtained by scattering techniques.

NR analysis indicated a significant amount of BBP segregation at the interface with a clear influence on the polymer interfacial width. While in qualitative agreement, the experimentally observed behavior, solvent interfacial excesses, and interfacial broadening are an order of magnitude than what is predicted by a polymer self-consistent mean-field theory (SCMF) for reasons that are as-yet unknown.

Our experimental results have potential practical implications that need verification. While an enhanced degree of entanglement at a pure polymer/polymer interface is synonymous with improved interfacial strength, it has not been determined whether the plasticizer induced effect will have a similar effect. In fact, a more mobile interface may increase the toughness of the interface and, depending on the molecular weights of the two polymers, induced a shift in the mode of interfacial fracture (for example, from chain scission to pull-out[4]).

A wide range of additives are added to commodity polymers during processing. While these additives are well-known to alter the blend morphology, an understanding of the mechanisms behind these processes are poorly understood and can be well served by these results. The results may also be of interest to a broader readership beyond polymer films, e.g., additive effects in solar cell research[28] or researchers working in the field of nanoparticle polymer composites.

References and Notes

(1) Lange, J.; Wyser, Y. *Packag. Technol. Sci.* **2003**, *16* (4), 149.
(2) Nakayama, Y. *Prog. Org. Coat.* **1998**, *33* (2), 108.
(3) Siepmann, F.; Siepmann, J.; Walther, M.; MacRae, R. J.; Bodmeier, R. *J. Controlled Release* **2008**, *125* (1), 1.
(4) Creton, C.; Kramer, E. J.; Hui, C. Y.; Brown, H. R. *Macromolecules* **1992**, *25* (12), 3075.
(5) Russell, T. P. *Annu. Rev. Mater. Sci.* **1991**, *21*, 249.
(6) Helfand, E.; Tagami, Y. *J. Chem. Phys.* **1972**, *56* (7), 3592.
(7) Shull, K. R.; Kramer, E. J. *Macromolecules* **1990**, *23* (22), 4769.
(8) Huang, C.; delaCruz, M. O. *Phys. Rev. E* **1996**, *53* (1), 812.
(9) Huang, C.; Delacruz, M. O.; Swift, B. W. *Macromolecules* **1995**, *28* (24), 7996.
(10) Lifschitz, M.; Freed, K. F. *J. Chem. Phys.* **1993**, *98* (11), 8994.
(11) Helfand, E. *Macromolecules* **1992**, *25* (6), 1676.
(12) Tang, H.; Freed, K. F. *J. Chem. Phys.* **1991**, *94* (9), 6307.
(13) Helfand, E.; Sapse, A. M. *J. Chem. Phys.* **1975**, *62* (4), 1327.
(14) Hong, K. M.; Noolandi, J. *Macromolecules* **1981**, *14* (3), 736.
(15) Clarke, C. J.; Jones, R. A. L.; Edwards, J. L.; Shull, K. R.; Penfold, J. *Macromolecules* **1995**, *28* (6), 2042.
(16) Monsanto Chemical Company, UK Patent number 969911.
(17) Payne, R. S.; Clough, A. S.; Murphy, P.; Mills, P. J. *Nucl. Instrum. Methods Phys. Res., Sect. B* **1989**, *42* (1), 130.
(18) Zeigler, J. F.; Biersek, H.; Littmark, U. *The Stopping and Range of Ions in Matter*; Pergamon: New York, 1985; Vol. *1*.
(19) Broseta, D.; Fredrickson, G. H.; Helfand, E.; Leibler, L. *Macromolecules* **1990**, *23* (1), 132.
(20) Crowley, T. L.; Lee, E. M.; Simister, E. A.; Thomas, R. K. In *The Use of Contrast Variation in the Specular Reflection of Neutrons from Interfaces*; Workshop on Methods of Analysis and Interpretation of Neutron Reflectivity Data, Argonne, IL, Aug 23−25, 1990; Elsevier Science Bv: Argonne, IL, 1990; p 143.
(21) Carelli, C.; Young, R. N.; Jones, R. A. L.; Sferrazza, M. *Nucl. Instrum. Methods Phys. Res., Sect. B* **2006**, *248* (1), 170.
(22) Sivia, D. S. *Philos. Mag.* **2007**, *87* (10), 1575.
(23) Sivia, D. S.; Hamilton, W. A.; Smith, G. S. In *Analysis of Neutron Reflectivity Data - Maximum-Entropy, Bayesian Spectral-Analysis and Speckle Holography*; Workshop on Methods of Analysis and Interpretation of Neutron Reflectivity Data, Argonne, IL, Aug 23−25, 1990; Elsevier Science Bv: Argonne, IL, 1990; p 121.
(24) Sivaniah, E.; Sferrazza, M.; Jones, R. A. L.; Bucknall, D. G. *Phys. Rev. E* **1999**, *59* (1), 885.
(25) Anastasiadis, S. H.; Russell, T. P.; Satija, S. K.; Majkrzak, C. F. *Phys. Rev. Lett.* **1989**, *62* (16), 1852.
(26) Fernandez, M. L.; Higgins, J. S.; Penfold, J.; Ward, R. C.; Shackleton, C.; Walsh, D. J. *Polymer* **1988**, *29* (11), 1923.
(27) Wang, X. C.; Sanchez, I. C. *Langmuir* **2007**, *23* (24), 12192.
(28) Hwang, I. W.; Cho, S.; Kim, J. Y.; Lee, K.; Coates, N. E.; Moses, D.; Heeger, A. J. *J. Appl. Phys.* **2008**, *104* (3), 9.